



Contents lists available at ScienceDirect

Spectrochimica Acta Part A: Molecular and Biomolecular Spectroscopy

journal homepage: www.elsevier.com/locate/saa

Synthesis and characterization of heterotrinnuclear bis (μ_2 -chlorido)dicopper (II) mono zinc(II) complexes derived from succinoyldihydrazones

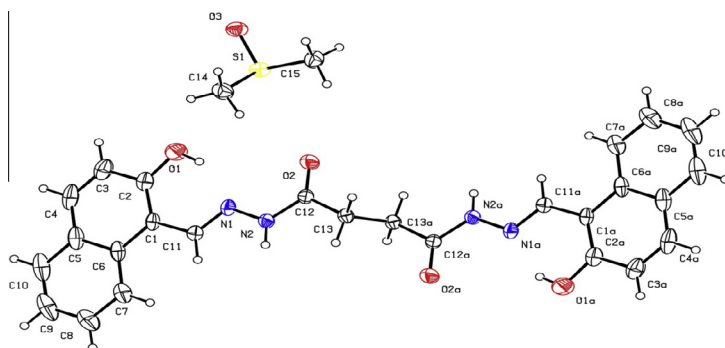
Rosmita Borthakur^a, Arvind Kumar^b, R.A. Lal^{a,*}^a Department of Chemistry, North Eastern Hill University, Shillong 793022, Meghalaya, India^b Department of Chemistry, Faculty of Science and Agriculture, The University of West-Indies, St Augustine, Trinidad and Tobago

HIGHLIGHTS

- Three new zinc (II)–copper (II) heterotrinnuclear complexes have been synthesized.
- The structure of the ligand H_4L^2 has been established by X-ray crystallography.
- The dihydrazone ligand is present in enol form in all of the complexes.
- Copper centre has tetragonally distorted octahedral stereochemistry.
- EPR parameters indicate that copper centre has doublet state as the ground state.

GRAPHICAL ABSTRACT

Three new heterotrinnuclear copper (II)–zinc (II) complexes having composition $[Cu_2Zn(L)(\mu_2-Cl)_2(H_2O)_6] \cdot 2H_2O$ ($H_4L = N, O$ donor schiff base ligands) were prepared and characterised by UV–vis, IR, magnetic moment and EPR spectroscopy. The electron transfer reactions for the complexes have been studied by cyclic voltammetry. Single crystal structure of H_4L^2 .



ARTICLE INFO

Article history:

Received 3 April 2013

Received in revised form 9 August 2013

Accepted 15 August 2013

Available online 30 August 2013

Keywords:

Heteropolymetallic complexes

Succinoyldihydrazones

Zinc (II)

Copper (II) complexes

Spectroscopic studies and cyclic voltammetric studies

ABSTRACT

Three new zinc (II)–copper (II) heterometallic trinuclear complexes of the composition $[ZnCu_2(L^n)(\mu_2-Cl)_2(H_2O)_6] \cdot 2H_2O$ ($H_4L^n = H_4L^1, H_4L^2, H_4L^3$) have been synthesized from substituted succinoyldihydrazones (H_4L^n) in methanol medium. The composition of the complexes has been established on the basis of data obtained from analytical, mass spectral studies and molecular weight determinations in DMSO. The structure of the ligand H_4L^2 has been established by X-ray crystallography. The structure of the complexes has been discussed in the light of molar conductance, magnetic moment, electronic, EPR, IR and FT-IR spectral studies. The molar conductance values for the complexes fall in the region 1.2 – $1.7 \text{ ohm}^{-1} \text{ cm}^2 \text{ mol}^{-1}$ in DMSO solution indicating that all of these are non-electrolyte. The magnetic moment values suggest weak M–M interaction in the structural unit of the complexes. The dihydrazone ligand is present in enol form in all of the complexes. Copper centre has tetragonally distorted octahedral stereochemistry. The EPR parameters of the complexes indicate that the copper centre has doublet state as the ground state. The electron transfer reactions of the complexes have been investigated by cyclic voltammetry.

© 2013 Elsevier B.V. All rights reserved.

* Corresponding author. Tel.: +91 0364 2722616.

E-mail address: ralal@rediffmail.com (R.A. Lal).

Introduction

Copper is a biologically important metal and occurs in enzymes and metalloproteins like ascorbate oxidase copper monooxygenase, copper dioxygenase, superoxide dismutase, cytochrome oxidase and blue oxidase [1]. In living organisms, it is often present in mono-, di-, or trinuclear assemblies. When blue copper site in multinuclear copper oxidases is substituted by a redox innocent mercuric ion, O₂-bond cleavage by the fully reduced trinuclear site is significantly impeded [2]. The multimetallic copper complexes are also important because of their relevance in the development of novel functional materials showing molecular ferromagnetism [3] and specific catalytic properties [4]. Homo- and hetero-trimetallic copper complexes offer the opportunities to test magnetic exchange models on more complicated systems. Copper (II) complexes find application as catalyst for the oxidation of alcohols into aldehydes and ketones [5].

Hydrazones are special kind of polyfunctional Schiff base ligands derived from condensation of organic acid hydrazines and o-hydroxy aromatic aldehydes and ketones [6–10] which have potential for yielding homo- and hetero-metallic complexes. The dihydrazones derived from condensation of succinoyldihydrazines and o-hydroxy-aromatic aldehydes and ketones are unique in the sense that their succinoyl fraction offers greater flexibility in three dimensional space because of their capability for free rotation about C–C single bond as compared to those in which the two hydrazone groupings are joined together either directly (oxaloyl) or through phenyl or pyridyl groups. Such dihydrazones, although, might exist in only one configuration in free state, in metal complexes can exist in staggered, anti-cis or syn-cis configuration [10]. The resulting dihydrazones contain salicylaldimine, 2-hydroxy-naphthalaldimine and 5-bromo-salicylaldimine in their molecular skeleton. Further, as we go from salicylaldimine dihydrazone to naphthalaldimine dihydrazone to 5-bromo-salicylaldimine dihydrazone, the bulkyness and electronegativity both increase in the same order. It is quite interesting to see how the properties of the complexes change as we go from one dihydrazone to next one.

A survey of literature reveals that although some isolated studies are available on metal complexes of succinoyldihydrazones [10] and related dihydrazones [6–10] yet the synthesis and characterization of heterotrinnuclear complexes of dihydrazones is quite meagre [11]. Moreover, a systematic study on trinuclear metal complexes of succinoyldihydrazones is absent to the best of our knowledge inspite of their highly flexible nature. In view of the above importance of copper complexes, absence of work on heterotrinnuclear complexes of succinoyldihydrazones and highly flexible polyfunctional nature of succinoyldihydrazones, it was of interest to synthesize the heterotrinnuclear copper complexes of the title dihydrazones (Fig. 1) and to characterize them by various physico-chemical and spectroscopic studies. Further, it was of

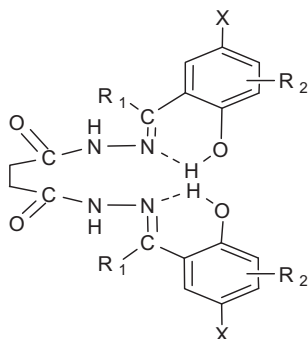


Fig. 1. Structure of ligands.

interest to investigate the electron transfer reactions of the complexes by cyclic voltammetry. The results of such an investigations are presented in this paper.

R ₁	R ₂	X	Dihydrazone ligand
H	H	H	Disalicylaldehydesuccinoyldihydrazone (H₄L¹)
H	5,6-benzo	H	Bis(2-hydroxy-1-naphthaldehyde) succinoyldihydrazone (H₄L²)
H	H	Br	Bis(5-bromosalicylaldehyde) succinoyldihydrazone (H₄L³)

Experimental

Materials

Zinc acetate dihydrate, copper chloride dihydrate, diethyl succinate, hydrazine hydrate, substituted salicylaldehyde and 2-hydroxy-1-naphthaldehyde were E-Merck, Qualigens, Hi-Media or equivalent grade reagents.

Instrumentation and measurement

Copper and zinc were determined by standard literature procedure [12]. Chloride was determined as AgCl [12]. C, H, N were determined by micro-analytical method using Perkin-Elmer, 2400 CHNS/O Analyser II. All conductance measurements were made at 1 kHz using Wayne Kerr B905 Automatic Precision Bridge. A dip-type conductivity cell having a platinised platinum electrode. The cell constant was determined using a standard KCl solution. Room temperature magnetic susceptibility measurements were made on a Sherwood Magnetic Susceptibility Balance MSB-Auto. Diamagnetic corrections were carried out using Pascals Constant [13]. Electronic spectra of the complexes were recorded in DMSO solution at $\sim 10^{-3}$ M concentration on a Perkin-Elmer Lambda-25 spectrophotometer. Electron paramagnetic resonance spectra of the complexes were recorded at X-band frequency on a Varian E-112 E-Line Century Service EPR spectrometer using TCNE ($g = 2.0027$) as an internal field marker. Variable temperature experiments were carried out with a Varian Variable Temperature accessory. Infrared spectra were recorded on a BX-III/FT-IR Perkin-Elmer Spectrophotometer in the range 4000–400 cm⁻¹ in KBr discs and 600–50 cm⁻¹ in CsI discs. The molecular weights of the complexes were determined in DMSO by freezing point depression method. Mass losses were determined by heating the complexes at 110 °C and 180 °C in an electronic oven. APCI mass spectra of the complexes were recorded on a water Zg 4000 Micromass Spectrometer in DMSO solution. Cyclic voltammetric measurements of the compounds in DMSO were done using a CH instruments Electrochemical analyzer under dinitrogen. The electrolytic cell comprises of three electrodes, the working electrode was a Pt disk while the reference and auxiliary electrodes were Ag/AgCl separated from the sample solution by a salt bridge; 0.1 mol L⁻¹, TBAP was used as the supporting electrolyte.

Molecular weight determination

The molecular weight of the complexes were determined in DMSO ($K_f = 4.07$) [14] as a solvent, by lowering of the freezing point of DMSO (f.p. 18.5 °C) using Beckman's freezing point depression instruments. The instrument consisted of a Beckman thermometer and a stirrer with a non-conducting handle of wood fitted into a tube through a rubber stopper fixed at its upper end. This tube was supported through a rubber stopper in a bigger glass

tube thoroughly purged with dry dinitrogen which acts as a dry dinitrogen jacket and ensures slow and uniform cooling of the inner tube. The outer tube is immersed in a 1,2-dimethyl-3-nitrobenzene (F. P. 15 °C) freezing bath contained in a glass jar. The jar was covered with a lid of plastic which carries three holes, one for inserting the inner tube, other for large metal stirrer and third for inserting the ordinary thermometer. The molecular weight apparatus was enclosed in a dry box that was constantly purged with dry nitrogen to minimize the error due to highly hygroscopic nature of DMSO. The different samples of the solutions were prepared in DMSO taking different amounts of complexes. All of the samples were placed in an entry port and purged overnight with dry dinitrogen before bringing them into the dry box. 20 g of DMSO was transferred into the thoroughly cleaned and dried freezing point tube purged with dry dinitrogen. About 0.6 g of the complex was accurately weighed and inserted into the DMSO solution. The tube was heated to dissolve the compound and then brought to room temperature. Finally, the upper surface of the liquid in the tube was purged with dry dinitrogen and then adjusted into the outer tube. The freezing point temperatures of the solvent and the solutions were directly measured with this apparatus through a magnifying glass fitted into the dry box.

X-ray crystallographic analysis of H_4L^2

The X-ray diffraction data were collected by mounting a single crystal of the sample on glass fibers. Oxford diffraction XCALIBUR-EOS diffractometer was used for the determination of cell parameters and intensity data collection at 273 K. Monochromating Mo $K\alpha$ radiation ($\lambda = 0.71073 \text{ \AA}$) was used for the measurements. The crystal structures were solved by direct methods using SHELXL-97 Program [15] and were refined by full matrix least-squares SHELXL-97 [16]. Non-hydrogen atoms were refined with anisotropic thermal parameters. Hydrogen atoms were placed into calculated positions and refined using a riding model.

Synthesis of compounds

The precursor monometallic zinc complexes $[Zn(H_2L^n)(H_2O)_2]$ ($H_4L^n = H_4L^1-H_4L^3$) were prepared by literature method [17].

Synthesis of $[ZnCu_2(L^n)(\mu_2-Cl)_2(H_2O)_6] \cdot 2H_2O$ [where $H_4L^n = H_4L^1(1), H_4L^2(2), H_4L^3(3)$]

$[Zn(H_2L^1)(H_2O)_2]$ (2.0 g; 4.43 mmol) was suspended in methanol (30 mL) and stirred vigorously to get a homogeneous suspension. This suspension was added into copper chloride dihydrate solution maintaining $[Zn(H_2L^1)(H_2O)_2]:CuCl_2 \cdot 2H_2O$ 1 molar ratio at 1:3 and was refluxed for 3 h which precipitated a green coloured compound. The compound was suction filtered in hot condition and washed several times with methanol (30 mL each time) followed by ether and finally dried over anhydrous $CaCl_2$.

The complexes **2** and **3** were also prepared by following the above procedure using $[Zn(H_2L^2)(H_2O)_2]$ (2.0 g; 3.28 mmol) and $[Zn(H_2L^3)(H_2O)_2]$ (2 g; 3.63 mmol) respectively, instead of $[Zn(H_2L^1)(H_2O)_2]$.

$[ZnCu_2(L^1)(\mu_2-Cl)_2(H_2O)_6] \cdot 2H_2O$ (1). Yield: 2.60 g (78%), M.p.: 210 °C
Anal.: Calc for $C_{18}H_{30}N_4O_{12}Cu_2ZnCl_2$ (%): Cu, 16.78; Zn, 8.63; C, 28.52; H, 3.96; N, 7.39; Cl, 9.36. Found: Cu, 16.39; Zn, 8.79; C, 28.90; H, 3.95; N, 7.72; Cl, 9.56. **Mol. Wt. (theo.): (757.49), exp.: (980 ± 50)**. Molar Conductance (DMSO, $\Omega^{-1} \text{ cm}^2 \text{ mol}^{-1}$): 1.7.

$[ZnCu_2(L^2)(\mu_2-Cl)_2(H_2O)_6] \cdot 2H_2O$ (2). Yield: 2.23 g (72%), M.p.: 290 °C
Anal.: Calc for $C_{26}H_{34}N_4O_{12}Cu_2ZnCl_2$ (%): Cu, 14.82; Zn, 7.63; C, 36.36; H, 3.97; N, 6.53; Cl, 8.27. Found: Cu, 15.13; Zn, 7.46;

C, 36.74; H, 4.01; N, 6.80; Cl, 8.05. **Mol. Wt. (theo.): (857.49), exp.: (1150 ± 55)**. Molar Conductance (DMSO, $\Omega^{-1} \text{ cm}^2 \text{ mol}^{-1}$): 1.5.

$[ZnCu_2(L^3)(\mu_2-Cl)_2(H_2O)_6] \cdot 2H_2O$ (3). Yield: 2.45 g (85%), M.p.: 270 °C
Anal.: Calc for $C_{18}H_{28}N_4O_{12}Br_2Cu_2ZnCl_2$ (%): Cu, 13.88; Zn, 7.14; C, 23.59; H, 3.06; N, 6.12; Cl, 7.75. Found: Cu, 13.53; Zn, 7.32; C, 23.93; H, 3.03; N, 5.91; Cl, 7.98. **Mol. Wt. (theo.): (915.49), exp.: (1250 ± 60)**. Molar Conductance (DMSO, $\Omega^{-1} \text{ cm}^2 \text{ mol}^{-1}$): 1.2.

Results and discussion

Structural description of ligand (H_4L^2)

Crystallographic data and refinement details for the structural analyses of the ligand (H_4L^2) is summarized in (Table 1). Selected bond lengths and bond angles are presented in (Table 2). A single unit cell with atom numbering scheme and atom connectivity of the ligand (H_4L^2) is shown in (Fig. 2). The X-ray single-crystal structure determination of ligand (H_4L^2) suggested that it was crystallized in monoclinic crystal system with space group P 21/c. The two procumbent naphthyl rings constitute a staggered configuration about the central $-CH_2-CH_2-$ bond and adopt an extended conformation (Fig. 2). The N(1)–C(11) bond length is 1.273. This bond length is shorter than the mean reported bond length for a single C–N bond (1.437 Å) and is very close to the mean bond length reported for a C=N double bond (1.289 Å). These data clearly reveal complete localization of the electron lone pair of N(1) atoms [18]. The two parts of the molecule have a centre of symmetry. The carbonyl groups have anti-configuration and there is an intramolecular hydrogen bonding between O(1)–H(1)···N(1) with bond length 2.55 Å to form six membered ring involving atoms O(1)–H(1)–N(1)–C(11)–C(1)–C(2). In addition, there are two intermolecular hydrogen bonds involving secondary N–H proton (N2) and oxygen of cocrystallized DMSO molecule (O3) [19] (Fig. S1). The mode of packing of the compound in stereo projection along b-direction is illustrated in (Fig. S2).

Table 1
 Crystal data and structure refinement for $[H_4L^2]$.

Empirical formula	$C_{30}H_{34}N_4O_6S_2$
Formula weight	610.75
Temperature (K)	293
Wavelength (Å)	0.71073
Crystal system, space group	Monoclinic, P 21/c
<i>Unit cell dimensions</i>	
a (Å)	20.119(2)
b (Å)	4.6311(3)
c (Å)	17.5223(18)
α (°)	90
β (°)	114.680(13)
γ (°)	90
Volume (Å ³)	1483.5(3)
Z, calculated density (Mg/m ³)	2
D_{calc} (g/cm ^{−3})	1.367
Absorption coefficient (mm ^{−1})	0.230
F(000)	644.0
Crystal size (mm)	0.31 × 0.31 × 0.30
Theta range for data collection (°)	3.1828–28.9516
Reflections collected/unique [R(int)]	3400/2044
Completeness to theta	29.02
Absorption correction	Multi-scan
Maximum and minimum	0.98345 and 1.00000
<i>Transmission</i>	
Refinement method	Full-matrix least-squares on F ²
Data/restraints/parameters	3400/0/198
Goodness-of-fit on F ²	0.983
Final R indices [I > 2σ(I)]	R1 = 0.0547, wR2 = 0.1330
R indices (all data)	R1 = 1067, wR2 = 0.1099
Largest diff. peak and hole	0.002 and 0.021

Table 2
Selected interatomic distances (Å) and bond angles (°) for the compound.

C(1)–C(2)	1.382	C(1)–C(11)	1.454
C(11)–N(1)	1.273	C(2)–C(3)	1.405
N(1)–N(2)	1.375	C(3)–C(4)	1.342
N(2)–C(12)	1.350	C(4)–C(5)	1.401
C(12)–C(13)	1.507	C(5)–C(6)	1.423
C(2)–O(1)	1.348	C(6)–C(7)	1.412
C(12)–O(2)	1.221	C(7)–C(8)	1.366
N(1)–O(1)	2.555	C(8)–C(9)	1.387
S(1)–C(15)	1.775	C(9)–C(10)	1.355
S(1)–O(3)	1.505	C(5)–C(10)	1.415
C(1)–C(6)	1.439		
C(1)–C(2)–O(1)	122.78	C(4)–C(5)–C(10)	121.84
C(2)–C(1)–C(11)	120.15	C(5)–C(10)–C(9)	121.24
O(1)–C(2)–C(3)	116.15	C(10)–C(9)–C(8)	120.07
C(1)–C(2)–C(3)	121.07	C(9)–C(8)–C(7)	120.71
C(2)–C(3)–C(4)	120.43	C(8)–C(7)–C(6)	121.34
C(3)–C(4)–C(5)	121.73	C(7)–C(6)–C(5)	117.62
C(4)–C(5)–C(6)	119.14	C(7)–C(6)–C(1)	123.57
C(6)–C(1)–C(11)	121.03	C(1)–C(11)–N(1)	120.90
C(11)–N(1)–N(2)	117.12	N(1)–N(2)–C(12)	120.15
N(2)–C(12)–C(13)	114.20	C(13)–C(12)–O(2)	122.30
C(12)–C(13)–C(13a)	110.23	C(14)–S(1)–O(3)	105.97
C(14)–S(1)–C(15)	98.02	C(15)–S(1)–O(3)	106.14

Synthesis of complexes

Synthesis of the heterometallic complexes were achieved by reaction of precursor zinc (II) complexes $[\text{Zn}(\text{H}_2\text{L}^n)(\text{H}_2\text{O})_2]$ with copper (II) chloride in methanol keeping precursor complex: $\text{CuCl}_2 \cdot 2\text{H}_2\text{O}$ molar ratio at 1:3. Green or brown solutions were formed rapidly, resulting in compounds which were characterized by elemental analysis, spectroscopic and electrochemical analysis. On the basis of various analytical, thermo-analytical and mass spectral data, the complexes have been suggested to have the stoichiometry $[\text{ZnCu}_2(\text{L}^n)(\text{Cl}_2)(\text{H}_2\text{O})_6] \cdot 2\text{H}_2\text{O}$ ($\text{L}^n = \text{H}_4\text{L}^1$, H_4L^2 and H_4L^3). The complexes melt with decomposition in the temperature range 210–290 °C. It is imperative to mention that the melting point of the complex **1** is less than that of the corresponding parent ligand. This may be related to higher covalent character of metal–ligand bond as compared to that of the ligand [20]. On the other hand, the melting point of other complexes are higher than those of the corresponding parent ligand. This suggests that the

metal–ligand bond in these complexes have more ionic character than those in the corresponding parent ligands. All of the complexes are insoluble in water and common organic solvents but are soluble in highly coordinating solvents such as DMSO and DMF. All of the complexes show weight loss corresponding to two water molecules at 110 °C, while six water molecules at 180 °C when heated in an electronic oven for 4 h. The weight loss corresponding to two water molecules at 110 °C suggests that these water molecules are present in the lattice structure of the complexes. The six water molecules lost at 180 °C suggest that they are present in the first coordination sphere around metal centre.

The vapours evolved at 110 °C and 180 °C in the complexes were passed through a trap containing copper sulphate which turned blue. This confirmed that the vapours in the complexes originated from water molecules.

An effort was taken up to crystallize the complexes in various solvent systems under different experimental conditions. Unfortunately, only amorphous compounds precipitated in all our efforts which prevented analysis of the complexes by X-ray crystallography.

Mass spectral studies

All of the complexes have been characterized by mass spectroscopy. The molecular ions along with their experimental and theoretical masses, for all the complexes have been given in (Table S1). The mass spectra for the complexes **1** and **2** are shown in (Figs. S3 and S4).

The complexes **1** to **3** show a peak at m/z value of 541.4, 717.9, 745.0, 1107.7 and 992.2, 1108.0 respectively. For the complex **1**, the peaks at m/z value of 541.4 and 717.9 are close to the mass of molecular ions $[\text{Cu}_2\text{ZnL}^1]^+$ (542.49) and $[\text{Cu}_2\text{Zn}(\text{H}_2\text{L}^1)(\text{DMSO})_2(-\text{H}_2\text{O})]^+$ (718.49), respectively. The molecular ion $[\text{Cu}_2\text{ZnL}^1]^+$ arises from the loss of both the chloride ions and all water molecules while the molecular ion $[\text{Cu}_2\text{Zn}(\text{H}_2\text{L}^1)](\text{DMSO})_2(\text{H}_2\text{O})]^+$ owes its origin in the loss of two chloride ion and five water molecules from the coordination sphere followed by coordination of two DMSO molecules to the metal centre. The origin of different molecular ion peaks in the mass spectra of the complexes **2** and **3** is understandable in the same way and hence their further discussion

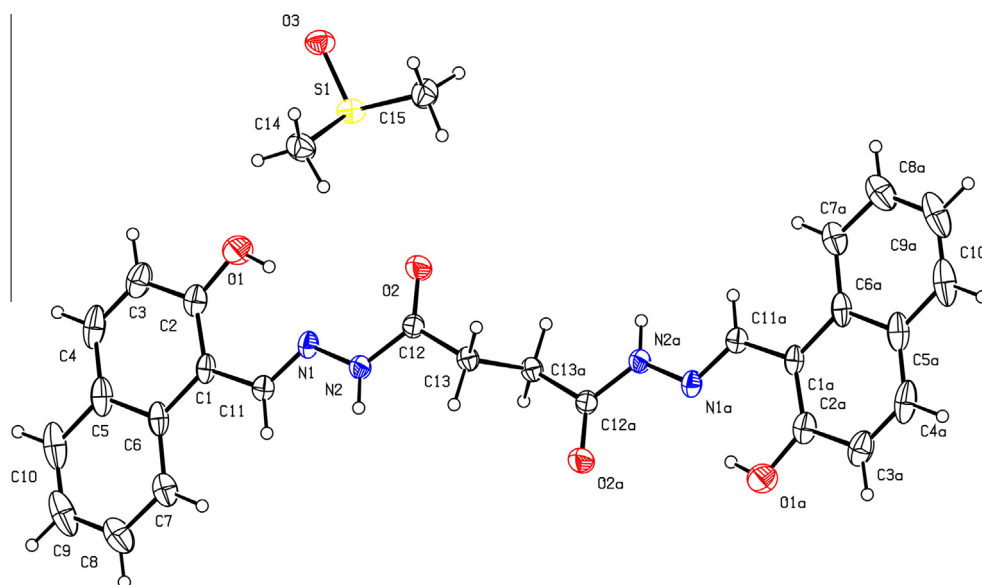


Fig. 2. Crystal structure of H_4L^2 with thermal ellipsoids plotted at 50% probability level.

seems redundant. The mass spectral data and their discussion suggest that all of the complexes are monomeric in character.

Molecular weight

The molecular weights of the complexes **1–3** have been determined in DMSO solution by freezing point depression method due to insolubility of the complexes in non-coordinating solvents. The experimental values of the molecular weights are (980 ± 50) , (1150 ± 55) and (1250 ± 60) , respectively. The experimental values of the molecular weights are very close to the theoretical values of 757.49, 857.49 and 915.49 for the monomeric formulation rather than the values 1514.98, 1714.98 and 1830.98 for the dimeric formulation. This suggests that the complexes are monomeric in nature. However, the experimental value of the molecular weight is considerably higher than the theoretical value calculated on the basis of the monomer formulation. This may be related partly to the break down of chlorido bridges in the complexes followed by coordination of DMSO molecules to the metal ions and partly due to substitution of some of the coordinated water molecules by DMSO molecules in the solution in all of complexes.

Molar conductance

The molar conductance values for the complexes in DMSO solution at 10^{-3} M dilution are in the range $1.2\text{--}1.7 \text{ ohm}^{-1} \text{ cm}^2 \text{ mol}^{-1}$. These values are consistent with their non-electrolytic nature in this medium [21].

Magnetic moment

The μ_{eff} value for the complexes are 2.12, 2.25 and 2.35 BM per molecular formula while per copper unit are 1.50, 1.59 and 1.66 BM, respectively. These values are less than the value of 2.44 BM for dinuclear copper (II) complexes and 1.73 BM for mononuclear complexes, respectively, involving no metal–metal interaction. These μ_{eff} values suggest considerably weak metal–metal interaction in the structural unit of the complexes. Such metal–metal interaction can be considered to occur only via superexchange mechanism through ligand backbone by inductive effect involving ligand bridging itself, the chloride bridging and enolate oxygen atom bridging via filled d^{10} -orbitals of the intervening zinc atom [22]. A minute examination of the magnetic moment value shows that μ_{eff} value increases in going from salicylaldehydato to 2-hydroxy-1-naphthaldehydato to 5-bromosalicylaldehydato complexes. This suggests that magnetic exchange is stronger in salicylaldehydato complex than that in 2-hydroxy-1-naphthaldehydato complex in which it is stronger than that in 5-bromosalicylaldehydato complex. This may be related to decreasing M–M interaction with increasing steric crowding as the size of the aromatic ring increases in going from salicylaldehyde to 2-hydroxynaphthaldehyde to 5-bromosalicylaldehyde complex. On the basis of the magnitude of magnetic moment, it may safely be concluded that both oxido as well as chlorido bridges are expected to be responsible for the lowering of the magnetic moment to the same extent.

Electron paramagnetic resonance

The X-band EPR spectra for the three trinuclear complexes have been recorded at RT and LNT in powder as well as DMSO glass at LNT. The various EPR parameters for the complexes have been set out in (Table S2). The EPR spectra for the complexes have been given in (Figs. S5–S7). The present ligands can react with the metal ions either in staggered configuration or syn-cis or anti-cis configuration [13,23]. The bonding of the ligands to the metal centre in

the staggered configuration in the present complexes is impossible, because they would, at the most, give rise to binuclear complexes only with the bivalent metal ions. If a trinuclear complex is to be formed, the only option available to the ligands is to exist in the cis-configuration and react with the metal ions [13,23]. Thus, the stereochemical consideration of the ligands suggests that their reaction with the metal ions in cis-configuration would give rise to trinuclear complexes.

The complexes **2** and **3** show an isotropic spectra in the solid-state at RT. The isotropic nature of the spectra of the complexes without any copper hyperfine splitting in the solid state at RT is due to intermolecular interaction [24]. However, when the complexes are sufficiently cooled to low temperature, intermolecular interactions are diminished in magnitude allowing the anisotropic spectra to appear with obvious hyperfine splitting in the g_{\parallel} region due to coupling of unpaired electron-spin with copper nucleus ($I = 3/2$). The spectra for the complexes look like an isolated copper (II) ion [25]. The hyperfine splitting constant for the complex **1** is 150 G. This value suggests either no interaction or very weak Cu··Cu interaction in the structural unit of the complex. The fact that the intensity of the signals decreased upon cooling from room temperature to 77 K confirms that the resonance occurs within the triplet excited state. The spin–spin interaction between the copper centres in the complexes can be considered to occur only via a superexchange mechanism involving enolate oxo-bridging and the chloride bridging via d^{10} orbitals of intervening zinc atom. The large metal–metal separation and long molecular pathway through zinc atom having d^{10} configuration between the copper centres are consistent with very weak exchange. Such weak exchange is typified by the compounds in which the two copper centres are separated by large distances with intervening 1, 2, 4, 5-tetrasubstituted benzene rings [26]. The weak exchange between Cu··Cu centres in these complexes is also corroborated by the room temperature magnetic moment studies on the complexes.

At 77 K, dimethyl sulphoxide glass spectra for the complexes show four weakly resolved peaks in the complexes **1** and **3** for the low-field side of the perpendicular region while two for the complex **2**. At LNT also, the spectra appear like an isolated copper (II) ion. The g_{\parallel} value for the complexes falls in the region 120–147 G which shows either weak interaction or no interaction at all between the two metal centres.

The tendency of A_{\parallel} to decrease with an increase of g_{\parallel} is an index of an increase in tetrahedral distortion in the square planar geometry in the coordination sphere of copper. However, in the case of octahedral or square pyramidal complexes, this has been related to the increased distortion in the equatorial plane. In order to quantify the degree of distortion in the copper (II) complexes, we have selected the factor $g_{\parallel}/A_{\parallel}$ obtained from EPR spectra which is considered as an empirical index of distortion in the equatorial plane [27]. It ranges between 105 and 135 for square planar equatorial configuration depending upon the nature of the coordinated atoms, highly distorted structure in the equatorial plane can have larger value [27]. The $g_{\parallel}/A_{\parallel}$ quotient for the complex **1** is 157.0 at LNT in the solid state, while for all of the complexes in DMSO glass at LNT, it lies in the range 171.2–200.4. The large value for $g_{\parallel}/A_{\parallel}$ quotients for the complexes reflects the increased distortion in the equatorial plane [28]. This clearly reflects a lower symmetry for the complexes [28].

Electronic spectroscopy

The free dihydrazones show bands in the regions ~ 292 , 327–340 and 330–382 nm, respectively. The bands in the regions ~ 292 and 327–340 nm are assigned to intra-ligand $\pi \rightarrow \pi^*$ transitions while the band in the region 330–382 nm to $n \rightarrow \pi^*$

transition. The band in the region 330–382 nm is characteristic of salicylaldehyde/naphthaldehyde part of the ligand [8e,8f].

In the solid state, the ligand bands appear as a single broad band having fine structure in the region 200–450 nm. However, they are not resolved, most probably, because they are overlapped with one another and are superimposed upon vibronic transitions. The complexes display a broad band centred in the region 710–775 nm (Table S2). This band is attributed to d–d transitions. The d–d transition occurs at around 800 nm in the octahedral complexes [29]. This band in octahedral complexes is considerably blue shifted due to Jahn–Teller distortion. The position of the d–d band and its shape suggests that the copper centres have distorted octahedral geometry in complexes.

The complexes display four well defined bands in the region 292–710 nm in solution (Table S2). The ligand band at ~292 nm splits into two bands. While one band remains almost unshifted in position, the other band shows red shift of about 20–29 nm in the complexes and appears in the region 316–332 nm. Further, the ligand band in the region 330–382 nm shows considerable red shift of about 34–53 nm on complexation and appears in the region 383–410 nm. Such a feature associated with the red shift of the ligand bands provides a good evidence for the chelation of dihydrazone to the metal centre. In DMSO solution, the complexes have absorbance maxima in the region 700–710 nm with molar extinction coefficient in the region $82\text{--}90\text{ dm}^3\text{ cm}^{-1}\text{ mol}^{-1}$. The d–d band in DMSO solution has slightly blue shifted as compared to that in solid state in complexes. This indicates interaction of DMSO molecule with metal centre in DMSO solution i.e. replacement of water molecules by DMSO molecules. However, the essential feature of the band in DMSO solution remains almost same as that in the solid state. This suggests that the stereochemistry of the complexes in solution as well as in the solid state remains same i.e. distorted octahedral (Fig. S11).

Infrared spectra

Some structurally significant IR bands for uncoordinated dihydrazone and complexes have been set out in (Table S3). The heterotrinnuclear Cu(II) and Zn(II) complexes **1–3** under study show characteristic bands due to ligation of ligands to the metal centre in the KBr-phase IR spectra. The IR spectra of the ligands show strong broad bands in the region $3184\text{--}3235\text{ cm}^{-1}$ and $3421\text{--}3446\text{ cm}^{-1}$ which are attributed to stretching vibrations of secondary –NH groups and phenolic/naphtholic –OH groups, respectively. In the IR spectra of the complexes, the band in the region $3184\text{--}3235\text{ cm}^{-1}$ due to νNH in free ligand is absent. Instead, all of the complexes show a strong broad band in the region $3420\text{--}3435\text{ cm}^{-1}$. The essential features of this band suggest it to be either due to lattice or coordinated water molecules. This shows that the dihydrazones coordinate to the metal centres in the enol form in the complexes. Another important and most characteristic feature of the IR spectra of the complexes is the absence of the band in the region $1659\text{--}1679\text{ cm}^{-1}$ due to >C=O group in the uncoordinated dihydrazones. This corroborates the fact that the ligand is present in enol form in the complexes. The present ligands show a very sharp band in the region $1615\text{--}1623\text{ cm}^{-1}$ which is assigned to stretching vibration of >C=N group. This band shifts to lower frequency by $15\text{--}27\text{ cm}^{-1}$ suggesting that >C=N group is involved in bonding to the metal centre. Another important feature of the IR spectra of the complexes is that they show a new weak to strong band in the region $1500\text{--}1512\text{ cm}^{-1}$. This band is characteristic of the presence of NCO– group [30]. The essential features associated with this band in the IR spectra of the complexes suggest that the dihydrazone undergoes enolization. The complexes show a band in the region $1267\text{--}1305\text{ cm}^{-1}$ which corresponds to the strong band in the region

$1240\text{--}1269\text{ cm}^{-1}$ in free dihydrazone ligand due to ν(C–O)(phenolic/naphtholic). The shift of this band to higher frequency by $10\text{--}43\text{ cm}^{-1}$ indicates bonding of phenolic/naphtholic oxygen atom to the metal centre via deprotonation [28]. The complexes show new bands in the region $500\text{--}546\text{ cm}^{-1}$ which are assigned to ν(M–O)(phenolate/naphtholate) [31]. The weak bands appearing in the region $456\text{--}477\text{ cm}^{-1}$ are attributed to ν(M–O)(enolic) stretching vibrations. The complexes show weak to medium intensity new bands in the regions $669\text{--}710$ and $447\text{--}490\text{ cm}^{-1}$, respectively. These bands are not visible in the spectra of the free ligands. Hence, they are assigned to arise due to oxo bridged metal atoms [32]. The position of the bands in the complexes is consistent with the involvement of enolate oxygen atoms in the bridge formation. The position of the bands in the complexes suggests that they originate from the formation of dibridge [33]. The band in the region $669\text{--}710\text{ cm}^{-1}$ is assigned to antisymmetric vibrations while the band in the region $447\text{--}490\text{ cm}^{-1}$ is assigned to symmetric vibrations of ($\text{M} \begin{array}{c} \diagup \diagdown \\ \text{O} \\ \diagdown \diagup \end{array} \text{M}$) group respectively.

The complexes show a new weak to medium intensity band in the region $210\text{--}228\text{ cm}^{-1}$. The terminal metal-chloride stretching vibrations are observed in the region $253\text{--}333\text{ cm}^{-1}$ in square planar chloride complexes while tetrahedral chlorido complexes show metal-chloride stretching vibrations in the region $306\text{--}355\text{ cm}^{-1}$. In the monomeric octahedral complexes, the terminal metal chloride stretching vibrations have been observed in the region $175\text{--}250\text{ cm}^{-1}$ [34]. The metal-chloride stretching vibration due to bridging chloride group in the polymeric octahedral complexes of first series transition metal complexes appears in the region $170\text{--}195\text{ cm}^{-1}$. The position of the copper – chloride stretching absorption band in the region $210\text{--}228\text{ cm}^{-1}$ in the present complexes indicates that they have distorted octahedral stereochemistry and that the chloride group is involved in bridge formation. However, νCu–Cl band appears in the region $210\text{--}228\text{ cm}^{-1}$ at slightly higher frequency than that normally observed in polymeric octahedral complexes of first series transition metal complexes may be related to monomeric character of the complexes.

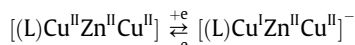
Cyclic voltammetry

The cyclic voltammograms of a 2 mM solution of the complexes have been recorded at a scan rate of 100 mV/s, 70 mV/s and 50 mV/s by cyclic voltammetric method in DMSO solution because of the solubility reasons in non-coordinating organic solvents (CH_3CN and CH_2Cl_2) with a 0.1 M tetra-n-butyl ammonium perchlorate (TBAP) as a supporting electrolyte. The potentials of the complexes were scanned in the potential range +2.4 to –2.4. The cyclic voltammetric data have been recorded in (Table S4). The cyclic voltammograms for the complexes at scan rates of 100 mV/s have been given in (Figs. S8–S10).

All of the complexes show three reductive and oxidative waves each in the forward and return scan, respectively. The reductive waves in the region –0.89 to –0.91 V and –1.37 to –1.56 V, respectively, do not have their counterparts in the oxidative scan. Hence, these waves are assigned to arise due to electron transfer reactions centred on the ligand. With the highly negatively charged dihydrazone ligand bonded to the metal centre, it is expected to make the reduction of these metal centres unfavourable, leading to quite negative Epc values [35]. Further, an oxidative wave at +0.75 V is observed in the complex $[\text{ZnCu}_2(\text{L}^2)(\mu_2\text{-Cl})_2(\text{H}_2\text{O})_6]\cdot 2\text{H}_2\text{O}$ **2**. This oxidative wave does not have its counterpart in the reductive scan. This suggests that the species produced corresponding to this oxidative wave is unstable in DMSO solution and reverts back to the original species. Hence, this oxidative wave is attributed to the oxidation of >C=N group in the ligand [36]. The remaining reductive and oxidative waves may be attributed to metal-centred electron transfer reactions. The first redox couple (Epc = –0.41 V

and $E_{pa} = -0.13$ V in complex **1**), ($E_{pc} = -0.36$ V and $E_{pa} = -0.24$ V in complex **2**) and ($E_{pc} = -0.43$ V and $E_{pa} = -0.21$ V in complex **3**) is either irreversible or quasi-reversible in nature. The peak potential separation for the complexes **1** to **3** are 280, 120 and 220 mV, respectively. This wave may be assigned to (L) $Cu^{II}Zn^{II}Cu^{II}/(L) Cu^{I}Zn^{II}Cu^{II}$, redox couple. The complex **2** shows another single oxidative wave at +0.34 V while the complexes **1** and **3** show additional oxidative waves at +0.10, +0.42 V and +0.11 and +0.38 V, respectively. These oxidative waves do not have their counterparts in the reductive waves. It appears that these oxidative waves arise, most probably, either from the species [(L) $Cu^{II}Zn^{II}Cu^{III}$] $^{1+}$ (in complex **2**) or from the species [(L) $Cu^{II}Zn^{II}Cu^{III}$] $^{1+}$ and [(L) $Cu^{III}Zn^{II}Cu^{III}$] $^{2+}$ (in complexes **1** and **3**), respectively. However, non-appearance of waves corresponding to these oxidative waves in the reductive scan suggests that they are highly unstable in DMSO solution and do not survive long. Hence, it is not possible to visualize the presence of Cu (III) containing species in the complexes.

The reductive and oxidative waves for first redox couples are separated from one another by 280 and 220 mV in complexes **1** and **3** respectively, suggesting that the redox processes are either irreversible or quasi-reversible. The high peak separation, most probably, originated from a slow heterogeneous electron exchange rate rather than from intervening homogeneous reaction [36]. In order to confirm that the electron transfer reaction in complexes **1** and **3** is a quasi-reversible metal-centred electron transfer reaction and the large separation between reductive and oxidative waves is due to slow heterogeneous electron exchange only, the cyclic voltammogram of the complexes were recorded at slower scan rates of 70 mV/s and 50 mV/s also. The point of crucial importance is that when the scan rate is decreased from 100 mV/s to 70 mV/s to 50 mV/s, the position of the waves corresponding to metal centred electron transfer reaction change and the separation between them decreases from 280 to 130 to 70 mV for the complex **1** and from 220 to 110 to 60 mV for the complex **3**, respectively. Similarly, the position of the metal centred electron transfer peaks also change and the separation between reductive and oxidative waves decreases from 120 to 90 to 60 mV in complex **2** as well. Such a cyclic voltammetric behaviour of the complexes shows that this is a quasi-reversible electron transfer process. However, this electron transfer process becomes completely reversible at a scan rate of 50 mV/s. The electron transfer reaction corresponding to these redox waves may be shown as below:



Conclusion

In the present study, we have synthesized three heterotrinary copper (II)–zinc (II) complexes of composition $[ZnCu_2(L^n)](\mu_2-Cl)_2(H_2O)_6 \cdot 2H_2O$ in excellent yields. All of the complexes are monomeric and non-electrolyte. The ligands are present in enol form in all of the complexes and function as tetrabasic hexadentate ligand coordinating to the metal centre through phenolate/naphtholate oxygen atoms, enolate oxygen atoms and azomethine nitrogen atoms. The EPR parameters indicate that the copper centre has $dx_{z^2} \rightarrow y^2$ orbital as the ground state. The electron transfer reactions of the complexes have been investigated by cyclic voltammetric studies. On the basis of interpretation of various physico-chemical and spectroscopic data, the complexes are suggested to have distorted octahedral structure, (Fig. S11).

Acknowledgements

Authors are thankful to the HEAD, SAIF, North Eastern Hill University, Shillong-793022, Meghalaya, India for recording NMR and

mass spectra, the Head, SAIF, IIT Bombay, India for recording EPR spectra. Authors express their heartfelt thanks to Prof. A.T. Khan, Department of Chemistry, IIT Guwahati, Assam, India for helping in recording the magnetic moment data.

Appendix A. Supplementary material

Crystallographic data (excluding structure factors) for the structures reported in this Article have been deposited with the Cambridge Crystallographic Data Centre (CCDC) as deposition nos. CCDC 912816 (for **H₄L²**). Copies of the data can be obtained, free of charge, on application to the CCDC, 12 Union Road, Cambridge CB2 1EZ, UK (fax, 44 (1223) 336 033; e-mail, deposit@ccdc.cam.ac.uk). Supplementary data associated with this article can be found, in the online version, at <http://dx.doi.org/10.1016/j.saa.2013.08.063>.

References

- [1] (a) E.I. Solomon, R.K. Szilagy, S.D. George, L. Basumallick, *Chem. Rev.* 104 (2009) 419–458; (b) E.I. Solomon, U.M. Sundaram, T.E. Machonkin, *Chem. Rev.* 96 (1996) 2563–2606.
- [2] D.J. Spira-Solomon, M.D. Allendorf, E.I. Solomon, *J. Am. Chem. Soc.* 108 (1990) 5318–5328.
- [3] D. Gatteschi, O. Kahn, J.S. Miller, F. Palacio (Eds.), *Magnetic Molecular Materials*, NATO-ASI Series E198, Kluwer Academic Publishers, Dordrecht, The Netherlands, 1991.
- [4] (a) G.A. Ardizzoia, S. Cenini, G. LaMonica, N. Masciocchi, M. Moret, *Inorg. Chem.* 33 (1994) 1458–1463; (b) O. Kahn, *Molecular Magnetism*, VCH Publishers, New York, 1993.
- [5] (a) M.V. Kirillova, Y.N. Kozlov, L.S. Shulpina, O.Y. Lyakin, A.M. Kirillov, E.P. Talsi, A.J.L. Pombeiro, G.B. Shulpin, *J. Catal.* 268 (2009) 26–38; (b) A.M. Kirillov, M.N. Kopylovich, M.V. Kirillova, M. Haukka, M.F.C.G. daSilva, A.J.L. Pombeiro, *Angew. Chem. Int. Ed.* 44 (2005) 4345–4349.
- [6] (a) J.D. Ranford, J.J. Vital, Y.M. Wang, *Inorg. Chem.* 37 (1998) 1226–1231; (b) N.A. Lalami, H.H. Monfred, H. Nou, P. Meyer, *Trans. Met. Chem.* 36 (2011) 669–677; (c) L. Zhao, V. Niel, L.K. Thompson, Z. Xu, V.A. Milway, R.G. Harvey, D.O. Miller, C. Wilson, M. Leech, J.A.K. Howard, S.L. Heath, *J. Chem. Soc. Dalton Trans.* (2004) 1446–1455.
- [7] (a) S. Ianelli, G. Minardi, C. Pelizzi, G. Pelizzi, R. Reverbari, C. Solinas, P. Tarasconi, *J. Chem. Soc. Dalton Trans.* (1991) 2113–2120; (b) A. Bacchi, L.P. Bhattaglia, M. Carcelli, C. Pelizzi, G. Pelizzi, C. Soliras, M.A. Zoroddu, *J. Chem. Soc. Dalton Trans.* (1993) 775–779; (c) A. Bonardi, S. Iaueli, C. Pelizzi, G. Pelizzi, C. Solinas, *Inorg. Chim. Acta* 232 (1995) 211–216.
- [8] (a) S. Pal, S. Pal, *J. Chem. Soc. Dalton Trans.* (2002) 2102–2108; (b) R. Dinda, P. Sengupta, S. Ghosh, H.M. Figge, W.S. Sheldrick, *J. Chem. Soc. Dalton Trans.* (2002) 4434–4439; (c) R. Dinda, P. Sengupta, S. Ghosh, W.S. Sheldrick, *Eur. J. Inorg. Chem.* (2003) 363–369; (d) A.R. Barreiro, R. Pedriclo, A.M.C. Noya, M.J. Romeiro, M. Varquez, L. Sorace, *New J. Chem.* 27 (2003) 1753–1759; (e) V.P. Singh, A. Katiyar, S. Singh, *J. Coord. Chem.* 62 (2009) 1336–1346.
- [9] (a) M.K. Singh, N.K. Kar, R.A. Lal, *J. Coord. Chem.* 61 (2008) 3158–3171; (b) M.K. Singh, N.K. Kar, R.A. Lal, *J. Coord. Chem.* 62 (2009) 1677–1689; (c) R.A. Lal, D. Basumatary, A.K. Dey, A. Kumar, *Trans. Met. Chem.* 32 (2007) 481–493; (e) A. Kumar, L.M. Mukherjee, A.N. Siva, A. Pal, S. Adhikari, K.K. Narang, M.K. Singh, *Polyhedron* 12 (1993) 2351–2354.
- [10] (a) R.A. Lal, S. Choudhury, A. Ahmed, R. Borthakur, M. Asthana, A. Kumar, *Spectrochim. Acta A* 75 (2010) 212–224; (b) R.A. Lal, D. Basumatary, A. Adhikari, A. Kumar, *Spectrochim. Acta Part A* 69 (706) (2008).
- [11] (a) O.B. Chanu, A. Kumar, A. Ahmed, R.A. Lal, *J. Mol. Struct.* 1007 (2012) 257–274; (b) O.B. Chanu, A. Kumar, A. Lemtur, R.A. Lal, *Spectrochim. Acta A* 96 (2012) 854–861.
- [12] I. Vogel, *A Textbook of Quantitative Inorganic Analysis including Elementary Instrumentation Analysis*, fourth ed., ELBS and Longmans, London, 1978.
- [13] A. Syamal, R.L. Dutta, *Elements of Magnetochemistry*, East-West Press. Pvt. Ltd., New Delhi, 1993.
- [14] J.A. Dean, *Langes Handbook of Chemistry*, fifth ed., McGraw Hill Inc., New Delhi, 1999.
- [15] G.M. Sheldrick, SHELXL-97, Program for X-ray Crystal Structure Solution, University of Gottingen, Gottingen, Germany, 1997.
- [16] G.M. Sheldrick, *Acta Crystallogr. Sect. A* 46 (1990) 467–473.
- [17] R.A. Lal, M. Chakraborty, O.B. Chanu, S. Choudhury, R. Borthakur, S. Copperfield, A. Kumar, *J. Coord. Chem.* 63 (2010) 1239–1251.

- [18] (a) A.G. Orpen, L. Brammer, F.H. Allen, O. Kennard, D.G. Watson, R. Taylor, *J. Chem. Soc. Dalton Trans.* (1989) S1–S83;
(b) W. Figueroa, M. Fuentella, C. Manzur, D. Canvillo, J.A. Mata, J.-R. Hamon, *J. Chilean. Chem. Soc.* 11 (2005) 1268–1275.
- [19] S. Akine, W. Dong, T. Nabeshima, *Inorg. Chem.* 45 (2006) 4677–4684.
- [20] W.G. Chu, H.F. Wang, Y.J. Guo, L.N. Zhang, Z.H. Han, Q.Q. Li, S.S. Fan, *Inorg. Chem.* 48 (2009) 1243–1249.
- [21] W.J. Geary, *Coord. Chem. Rev.* 7 (1971) 81–122.
- [22] (a) L. Gutierrez, G. Alzuet, J. A Real, J. Cano, J. Borrás, A. Casteineiras, *Inorg. Chem.* 39 (2000) 3608–3614;
(b) M.G. Alvarez, G. Alzuet, J. Borrás, B. Macías, A. Castineiras, *Inorg. Chem.* 42 (2003) 2992–2998.
- [23] A. Kumar, R. Borthakur, A. Koch, O.B. Chanu, S. Choudhury, A. Lemtur, R.A. Lal, *J. Mol. Struct.* 999 (2011) 89–97.
- [24] L. Banci, A. Bencini, B. Gatteschi, *Inorg. Chem.* 22 (1983) 4018–4021.
- [25] I. Castro, J. Sletten, J. Faus, M. Julve, Y. Journaux, F. Lloret, S. Alvarez, *Inorg. Chem.* 31 (1992) 1889–1894.
- [26] S.K. Mandal, L.K. Thompson, M.J. Newlands, E.J. Gabe, F.L. Lee, *Inorg. Chem.* 29 (1990) 3556–3561.
- [27] S.S. Tandon, L.K. Thompson, J.N. Bridson, J.C. Dewan, *Inorg. Chem.* 33 (1994) 54–61.
- [28] A. Syamal, K.S. Kale, *Inorg. Chem.* 18 (1979) 992–995.
- [29] B.N. Figgis, *Introduction to Ligand Fields*, Wiley, 1966.
- [30] M. Mashiuca, *Bull. Chem. Soc. Japan* 35 (1962) 2020–2026.
- [31] G.-C. Percy, D.A. Thornton, *J. Inorg. Nucl. Chem.* 34 (1972) 3369–3376.
- [32] (a) R. Lozano, A. Doadrio, A.L. Doadrio, *Polyhedron* 1 (1982) 163–167;
(b) W.E. Newton, J.L. Corbin, D.C. Bravard, J.E. Searles, J.W. Mc-Donald, *Inorg. Chem.* 13 (1974) 1100–1104.
- [33] J. Sanders-Loehr, W.D. Wheeler, A.K. Shiemke, B.A. Averill, T.M. Loehr, *J. Am. Chem. Soc.* 111 (1989) 8084–8093.
- [34] (a) K. Nakamoto, *Infrared and Raman Spectra of Inorganic and Coordination Compounds*, fourth ed., John Wiley & Sons, New York, 1986;
(b) J.R. Ferraro, *Low-Frequency Vibrations of Inorganic and Coordination Compounds*, Plenum Press, New York, 1971.
- [35] (a) B.M. Gatehouse, S.E. Livingstone, R.S. Nyholm, *J. Chem. Soc.* 22 (1957) 4222–4225;
(b) B.M. Gatehouse, S.E. Livingstone, R.S. Nyholm, *J. Inorg. Nucl. Chem.* 8 (1958) 79–86;
(c) N.F. Curtis, Y.M. Curtis, *Inorg. Chem.* 4 (1965) 804–809;
(d) S.A. Cameron, S. Brooker, *Inorg. Chem.* 50 (2011) 3697–3706.
- [36] H. Okawa, M. Koikawa, S. Kida, *J. Chem. Soc. Dalton Trans.* (1988) 641–645.